Quantifying Eddy Generation and Dissipation in the Jet Response to Upper- versus Lower-level Thermal Forcing

Yu Nie,[a] Yang Zhang,[b] Gang Chen,[c] and Xiu-Qun Yang[b]

[a] *Laboratory for Climate Studies, CMA-NJU Joint Laboratory for Climate Prediction Studies, National Climate Center, China Meteorological Administration, Beijing, China*

[b] *CMA-NJU Joint Laboratory for Climate Prediction Studies, Institute for Climate and Global Change Research, School of Atmospheric Sciences, Nanjing University, Nanjing, China*

[c] *Department of Earth and Atmospheric Sciences, University of California, Los Angeles, Los Angeles, California, USA*

Corresponding author: Yang Zhang, yangzhang@nju.edu.cn

Early Online Release: This preliminary version has been accepted for publication in *Journal of the Atmospheric Sciences* cited, and has been assigned DOI 10.1175/JAS-D-21-0307.1.The final typeset copyedited article will replace the EOR at the above DOI when it is published.

ABSTRACT: The relative roles of upper- and lower-level thermal forcing in shifting the eddy driven jet are investigated using a multi-level nonlinear quasi-geostrophic channel model. The numerical experiments show that the upper-level thermal forcing is more efficient in shifting the eddy-driven jet. The finite-amplitude wave activity diagnostics of numerical results show that the dominance of the upper-level thermal forcing over the lower-level thermal forcing can be understood from their different influence on eddy generation and dissipation that affects the jet shift. The upper-level thermal forcing shifts the jet primarily by affecting the baroclinic generation of eddies. The lower-level thermal forcing influences the jet mainly by affecting the wave breaking and dissipation. The former eddy response turns out to be more efficient for the thermal forcing to shift the eddy-driven jet.

Furthermore, two quantitative relationships based on the imposed thermal forcing are proposed to quantify the response of both eddy generation and eddy dissipation, and thus to help predict the shift of eddy-driven jet in response to the vertically non-uniform thermal forcing. By conducting the overriding experiments in which the response of barotropic zonal wind is locked in the model and a multi-wavenumber theory in which the eddy diffusivity is decomposed to contributions from eddies and mean flow, we find that the eddy generation response is sensitive to the vertical structure of the thermal forcing and can be quantified by the imposed temperature gradient in the upper troposphere. In contrast, the response of eddy diffusivity is almost vertically independent of the imposed forcing, and can be quantified by the imposed vertically-averaged thermal wind.

Accepted for publication in *Journal of the Atmospheric Sciences*. DOI 10.1175/JAS-D-21-0307.1

SIGNIFICANCE STATEMENT: Climate models predict enhanced warming over tropical upper-troposphere and Arctic surface in response to greenhouse gas increases, which has competing effects on the latitudinal shift of eddy-driven jet and thus requires a better understanding of the relative roles of upper- and lower-tropospheric thermal forcing for future climate projection. We make a new quantitative comparison on responses of eddy generation and dissipation that sustain the jet shift and relate them to the imposed thermal forcing. This approach extends the fundamental eddy closure topic from vertically uniform situation to vertically non-uniform forcing. These quantitative relationships are also helpful for better understanding and predicting the jet and storm track variabilities under other forms of thermal forcing (e.g., SST front, aerosols, latent heat release).

1. Introduction

Climate models predict that the warming of the troposphere in response to greenhouse gas forcing will not be uniform, exhibiting two hot spots, with one centered in the upper troposphere in the tropics and a second concentrated in the lower troposphere in the polar regions. The stronger warming over those two regions alters the spatial distribution of meridional temperature gradient in opposite direction in upper and lower troposphere, which, indicated by previous studies (Harvey et al. 2014; Shaw et al. 2016; Robert et al. 2019), has competing effects on the midlatitude atmospheric circulation and variability. The upper-level warming over the tropics has been shown to induce a poleward shift of storm tracks (Chang et al. 2012) and eddy-driven jet by raising the tropopause and high clouds (Lorenz and DeWeaver 2007; Li et al. 2019), accelerating the eddy phase speed (Chen and Held 2007), increasing the static stability (Lu et al. 2008; Yuval and Kaspi 2020), increasing the eddy length scale (Kidston et al. 2011), altering the subtropical irreversible potential vorticity (PV) mixing (Butler et al. 2011; Lu et al. 2013) and wave activity dissipation (Chen et al. 2013; Sun et al. 2013). However, observational and modeling studies suggest that the Arctic surface warming always results in an equatorward shift of the eddy-driven jet, associated with the weakening of the westerlies in high latitudes (Butler et al. 2010; Deser et al. 2016; Burrows et al. 2017). Thus, the final destination of the eddy-driven jet in the future climate could be "a tug of war" between the impacts of upper- and lower-level meridional temperature gradient (Deser et al.

Accepted for publication in *Journal of the Atmospheric Sciences*. DOI 10.1175/JAS-D-21-0307.1

2015), and understanding the relative roles of upper- and lower-level thermal forcing in shifting the eddy-driven jet has important implication for future climate projection.

Using a three-layer quasi-geostrophic model, Held and O'Brien (1992) examined the sensitivity of baroclinic eddy fluxes to the vertical structure of the background temperature gradient. They found that the strength of eddy fluxes, especially the eddy heat flux, are more sensitive to lower- than upper-level temperature gradient. Pavan (1996) used a multi-layer quasi-geostrophic model to better simulate the eddy dynamics and supported the results of Held and O'Brien (1992) by showing that the strength of eddy potential vorticity flux is more sensitive to the lower-level temperature gradient. He further interpreted this result as a consequence of the shallow eddies, which are confined in the lower levels with small vertical depth thus not affected by a change in the upper-level temperature gradient. Yuval and Kaspi (2016) refreshes the understanding of the topic by emphasizing the important role of the upper-level temperature gradient. Using an idealized global circulation model, the authors found that the strength of eddy activity, especially the baroclinic growth, is dominated by the upper tropospheric temperature gradient. They attributed this result to the large temperature gradient concentrated in upper levels, as in a 1D Eady-like model, the eddy growth rate is more sensitive to changes in regions of larger temperature gradient. All these previous studies have focused on sensitivities of the baroclinic eddy growth or the eddy PV flux. However, the response of the eddy-driven jet is more directly related to the eddy momentum flux convergence as suggested by Pfeffer (1987). The relative importance of upper- versus lower-level temperature gradient in forcing the eddy momentum flux remains unclear.

Besides the baroclinic growth of wave activity, the response of the eddy momentum flux to a given forcing is strongly affected by the meridional wave propagation and breaking aloft (Chang 1998; Barnes and Thompson 2014). The study by Thorncroft et al. (1993) has illustrated the sensitivity of the eddy momentum flux to the refractive index in the barotropic decay stage of an idealized baroclinic eddy life cycle. Kug and Jin (2009) and Ren et al. (2009) demonstrated the importance of eddy deformation by the background barotropic wind in shaping the eddy momentum flux. In all those processes, eddy deformation and its nonlinear breaking result in irreversible PV mixing, with the eddy activity dissipated at smaller scales. The irreversible changes in eddy activity are key to the balanced response in eddy momentum flux, whereas transient and reversible fluctuations in wave activity has a small net effect.

Accepted for publication in *Journal of the Atmospheric Sciences*. DOI 10.1175/JAS-D-21-0307.1

With the aid of the framework of finite-amplitude wave activity (FAWA) introduced by Nakamura and Zhu (2010), both the eddy growth and eddy dissipation processes that balance the eddy momentum flux are quantified and diagnosed. Nie et al. (2014), using this formalism, identified the strong association between eddy dissipation processes and the latitudinal shift of eddy-driven jet on intra-seasonal time scale. Studies by Nie et al. (2016) and Xiao et al. (2016) further suggest that those nonlinear eddy dissipation processes play a dominant role in sustaining the shift of the eddy-driven jet in response to the lower-level thermal forcing. Those studies raise a further question for understanding the relative importance of the upper and lower level thermal forcing in the jet shift: which of eddy growth or eddy dissipation is the dominant process associated with the change of eddy momentum flux convergence in response to upper- and lower-level thermal forcing? In addition, how can one quantify the relative contribution of the eddy generation and eddy dissipation in response to the imposed thermal forcing?

This study, as a continuation of Nie et al. (2016), aims to address the above questions by carrying out groups of sensitivity experiments to the upper- and lower-level thermal forcing. The numerical results are compared and analyzed through the FAWA diagnostic to disentangle and quantify the changes in eddy growth versus dissipation that accompany the response of eddy-driven jet. Our study shows that, in all the sensitivity experiments, the upper-level thermal forcing is more efficient in shifting the eddy-driven jet. The dominance of the upper-level thermal forcing over the lower-level forcing can be understood from their different influence on eddy generation and eddy dissipation responses that affect the jet shift. Through overriding experiments and a multi-wavenumber theory, we find that the eddy generation response is sensitive to the vertical structure of the thermal forcing and can be quantified by the imposed temperature gradient in the upper troposphere. In contrast, the eddy dissipation response is almost vertically independent of the imposed forcing, and can be quantified by the imposed vertically-averaged zonal wind.

The structure of the paper is assigned as follows. Section 2 outlines the model framework, experiments setup and methodology. The equilibrated responses of sensitivity runs are compared in Section 3. The eddy generation and dissipation responses that contribute to the jet response are diagnosed through FAWA analysis, and further quantified through overriding experiments and multi-wavenumber theory in Section 4. Summary and discussions are presented in Section 5.

Accepted for publication in *Journal of the Atmospheric Sciences*. DOI 10.1175/JAS-D-21-0307.1

2. Experiments design and analysis methods

a. The β plane multi-layer QG model

We use for this study a β-plane multi-layer quasi-geostrophic(QG) channel model with fixed static stability close to the observation (Zhang et al. 2009), with the Coriolis parameter f_o at the channel center and the latitudinal variation of the Coriolis parameter β all set to be the values at latitude $45°N$. This model simulates a pure eddy driven jet symmetric about the mid-channel, and ignores the spherical geometry effect on the asymmetry of wave dynamics, which may also play a role in the eddy sensitivity to the thermal forcing. This is one of the simplest environments to study the change of eddy activity and eddy driven jet in response to the vertical structure of the imposed thermal forcing, which does not consider the influence of spherical geometry and subtropical jet on the response of eddy driven jet. The framework and control parameters are the same as in Zhang et al. (2012) and Nie et al. (2016), with 156 km by 156 km horizontal resolution and 17 levels in the vertical. Model simulations with finer horizontal resolutions are also conducted to establish the robustness of the results. The model is governed by a potential vorticity equation, which is forced by diabatic heating H and damped by frictional dissipation $\mathbf{F_r}$. The diabatic heating in this work is contributed by the radiative convective heating H_r which is parameterized by the Newtonian relaxation to a target "radiative convective equilibrium (RCE)":

$$H_r = C_p \frac{T_e - T}{\tau_r}, \tag{1}$$

in which T_e denotes the RCE state temperature and $\tau_r = 40$ days, denoting the newtonian relaxation time scale. The potential temperature of the RCE state in the troposphere is specified as

$$\theta_e^+(y,p) = \begin{cases} \frac{\Delta_e}{2} & 0 \le y - y_0(p) < L/4 \\ \frac{\Delta_e}{2} sin[\frac{\pi(y-y_0(p))}{L/2}] & L/4 \le y - y_0(p) \le 3L/4 \\ -\frac{\Delta_e}{2} & 3L/4 < y - y_0(p) \le L \end{cases} \tag{2}$$

where $\theta_e = \theta_e^+ + \overline{\theta_e}^{xy}$. $\overline{\theta_e}^{xy}$ denotes horizontally averaged target state potential temperature, which is fixed and specified to be 280 K, close to the observed global averaged surface temperature. $\Delta_e = 43K$, denoting the temperature difference across the channel width L. In the stratosphere,

Accepted for publication in *Journal of the Atmospheric Sciences*. DOI 10.1175/JAS-D-21-0307.1

the potential temperature gradient of the RCE state is set to one tenth of that in the troposphere and of opposite sign. The results presented in this study are robust for moderate change of the background target state temperature gradient (results not shown). Note that the vertical profile of the static stability can affect the results. An extreme case for this situation is the stratosphere, in which the atmospheric response is strongly suppressed with the very stable stratification, which is out of the scope of this study. In this study, the background lapse rate is set to 7 K/km in the troposphere and zero in the stratosphere, close to the observation. A linearized bulk form surface sensible heat flux is also included in the model to act on the atmosphere at a time scale of few days. $F_{sh} = -C_{dt} c_p \rho_s (\theta_{air} - \theta_{sea})$, where C_{dt} is the drag coefficient and ρ_s is the surface air density. The sea surface potential temperature θ_{sea} is kept fixed as the RCE state surface potential temperature. We assume that the first model level is well-mixed so that the surface air potential temperature θ_{air} is equal to the potential temperature at the first level, which is 32 hPa above the surface. Frictional dissipation $\mathbf{F_r}$ is parameterized as $\mathbf{F_r} = g\frac{\partial \tau_m}{\partial p}$, where τ_m is the shear stress and set as $\tau_m = -c_d \mathbf{v_s}$ at the surface level ($\mathbf{v_s}$ denotes the surface wind). Sensitivity tests have been conducted to guarantee that conclusions made in this study are not sensitive to the detailed boundary layer setting in the model. More details of the model configuration and parameters can refer to Zhang et al. (2009, 2012) and Nie et al. (2016).

b. Experiments setup

In this study, the atmospheric response to upper- versus lower-level thermal forcing is compared through groups of sensitivity experiments, in which the potential temperature in the RCE state is modified. We start with a control (CTL) run with $y_0(p) = 0$, in which, as shown in Fig. 1a, both the upper- and lower-level temperature gradient are peaked at the channel center. Then sensitivity experiments are conducted by systematically displacing the latitude of the maximum $\partial T_e/\partial y$ away from the channel center at a given vertical level. This is achieved by varying the center of the baroclinic zone $y_0(p)$ in Eq.(2). Since the β-plane model neglects the spherical effects with its dynamics symmetric about the channel center, the shift direction of the thermal forcing does not matter and enables direct dynamical comparison of the response of upper versus lower level forcing. Thus, we set the upper- and lower-level thermal forcing all displaced poleward for comparing the extent of the resultant jet shift. Specifically, we set

Accepted for publication in *Journal of the Atmospheric Sciences*. DOI: 10.1175/JAS-D-21-0307.1

$$y_0(p) = \begin{cases} \frac{\Delta y}{2}[cos(\frac{p-p_c}{\delta p}\pi)+1] & |\frac{p-p_c}{\delta p}| \le 1 \\ 0 & |\frac{p-p_c}{\delta p}| > 1 \text{ or } p < p_t \end{cases} \quad (3)$$

where p_c is the vertical level in which the center of the baroclinic zone is maximal displaced and p_t=312.5 hPa is the tropopause level, Δy denotes the distance of the latitudinal displacement of the baroclinic zone at p_c, and δp denotes the vertical extent of the displaced baroclinic zone. As this study aims to investigate the tropospheric dynamics, no thermal perturbation is added in the stratosphere. Three groups of sensitivity studies: UP runs, LOW runs and Vertical runs are carried out. In the UP experiments, as shown in Fig. 1b, p_c is set at the tropopause, with the center of the upper tropospheric baroclinic zone shifted gradually poleward while the lower-level baroclinic zone is kept at the center of the channel. For comparison, the LOW experiments are designed as in Fig. 1c, in which p_c is set at the surface, with the center of the lower level baroclinic zone shifted gradually poleward while the upper level baroclinic zone is kept unchanged. In both UP and LOW experiments, four sensitivity runs are carried out respectively by increasing Δy with an increment of 625 km. The detailed values of parameters used in each run of the UP/LOW experiments are listed in Table 1.

In addition to the thermal forcing peaked at the tropopause and surface, another group of experiments, denoted "Vertical runs", are conducted to investigate the sensitivity of the atmospheric response to thermal forcing peaked at different vertical levels (Figs. 1d-f). As listed in Table 1, 10 sensitivity runs are carried out by setting the center level of the latitudinal displacement of the baroclinic zone from 1000 hPa to 437.5 hPa with a decrement of 62.5 hPa. To better disentangle the different influence of the heating level, δp is set as 250 hPa in the Vertical runs. The conclusions of the Vertical runs all hold for deeper extents of the displaced baroclinic zone (results not shown).

Each simulation is spun up for at least 1000 days and then integrated for an additional 5000 days for analysis. The equilibrated response is defined as the difference between the equilibrated states in the perturbed run and the control run.

c. Analysis method: the Finite-Amplitude Wave Activity diagnostics

This study investigates the response of a single midlatitude eddy driven jet to the upper versus lower level thermal forcing, which is primarily driven by the change in the vertically averaged

Accepted for publication in *Journal of the Atmospheric Sciences*. DOI 10.1175/JAS-D-21-0307.1

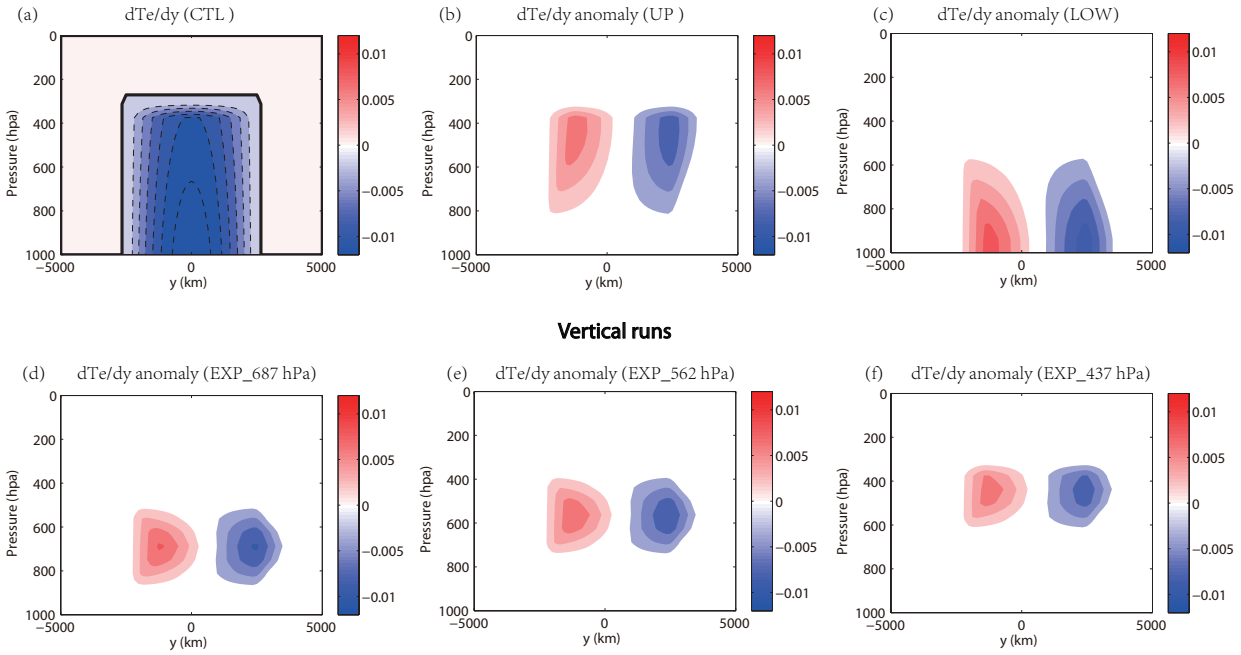

FIG. 1. (a) Profile of the target state temperature gradient $\partial[T_e]/\partial y$ as a function of pressure and latitude in the standard CTL run. (b)-(c) Vertical and latitudinal structure of the anomalous $\partial[T_e]/\partial y$ added in the (b) UP and (c) LOW runs associated with a latitudinal displacement of $\partial[T_e]/\partial y$ by 1250 km. (d)-(f) are same as (b)-(c) but for the Vertical runs with imposed forcing centered at (d) 687.5 hPa, (e) 562.5 hPa and (f) 437.5 hPa, respectively. Contour interval is 0.002 Kkm^{-1}. The thick black contour in (a) denotes the zero line.

convergence of eddy momentum flux for jet variability (Lorenz and Hartmann 2001, 2003). The response of a subtropical jet to thermal forcing is not considered. Since the eddy momentum flux convergence is mostly concentrated in the upper troposphere, the response of the eddy-driven jet is greatly governed by the dynamics in the upper levels (Nie et al. 2014). We employ the FAWA framework (Nakamura and Solomon 2010) instead of conventional Transformed Eulerian Mean (TEM) framework to investigate the eddy momentum response as in Chen et al. (2013) and Sun et al. (2013). First and most importantly, the FAWA framework enables to elucidate the relative importance of eddy growth and eddy dissipation (i.e., the source and sink of wave activity) that balances the response of eddy momentum flux convergence, which are not easy to assess under the TEM. Second, even for the local zonal wind variation (i.e. the upper level jet), previous studies have suggested that the zonal wind acceleration is better related to the eddy momentum flux convergence than the local Eliassen-Palm (E-P) flux divergence in the TEM, since it is determined by a small

Accepted for publication in *Journal of the Atmospheric Sciences*. DOI 10.1175/JAS-D-21-0307.1.

TABLE 1. Values of the parameters used in CTL run and sensitivity runs. Columns indicate the name of the experiment, latitudinal displacement of the baroclinic zone with the imposed anomalous thermal forcing, vertical center of the anomalous thermal forcing, and vertical extent of the anomalous thermal forcing, respectively.

EXPERIMENT	latitudinal displacement Δy	vertical center of imposed forcing p_c	vertical extent of imposed forcing δp
CTL Run	0 km		
LOW Run :			
LOW_625km	**625** km	1000 hPa	687.5 hPa
LOW_1250km	**1250** km	1000 hPa	687.5 hPa
LOW_1875km	**1875** km	1000 hPa	687.5 hPa
LOW_2500km	**2500** km	1000 hPa	687.5 hPa
UP Run :			
UP_625km	**625** km	312.5 hPa	687.5 hPa
UP_1250km	**1250** km	312.5 hPa	687.5 hPa
UP_1875km	**1875** km	312.5 hPa	687.5 hPa
UP_2500km	**2500** km	312.5 hPa	687.5 hPa
Vertical Run :			
$EXP\_1000hPa$	1250 km	**1000** hPa	250 hPa
$EXP\_937.5hPa$	1250 km	**937.5** hPa	250 hPa
EXP_875hPa	1250 km	**875** hPa	250 hPa
$EXP\_812.5hPa$	1250 km	**812.5** hPa	250 hPa
EXP_750hPa	1250 km	**750** hPa	250 hPa
$EXP\_687.5hPa$	1250 km	**687.5** hPa	250 hPa
EXP_625hPa	1250 km	**625.0** hPa	250 hPa
$EXP\_562.5hPa$	1250 km	**562.5** hPa	250 hPa
EXP_500hPa	1250 km	**500.0** hPa	250 hPa
$EXP\_437.5hPa$	1250 km	**437.5** hPa	250 hPa

difference between the Coriolis force on the residual circulation and the E-P flux divergence (Pfeffer 1987). Finally, our method is related to the parameterization of eddy momentum flux in a 2D model, in which eddy momentum flux is quantified by the difference between eddy diffusions of PV and potential temperature (Stone and Yao 1987).

In the FAWA formalism, the budget contributed to the convergence of the eddy momentum flux can be written as in Chen et al. (2013) and Nie et al. (2014):

$$M \equiv -\frac{\partial([u^*v^*])}{\partial y} = \underbrace{-\frac{\partial}{\partial p}\left(\frac{f[v^*\theta^*]}{\partial\theta_s/\partial p}\right)}_{eddy\,generation} \underbrace{-k_{eff}\frac{\partial Q}{\partial Y}}_{eddy\,dissipation} -\frac{\partial A}{\partial t} + \Delta\Sigma, \tag{4}$$

Accepted for publication in *Journal of the Atmospheric Sciences*. DOI 10.1175/JAS-D-21-0307.1

in which [ ] and * denote zonal-mean and deviation from zonal-mean, respectively. The first term on the right-hand-side (RHS) is the vertical differential of the eddy meridional heat flux divided by the static stability parameter. It represents the contribution from the baroclinic eddy generation (i.e. the poleward eddy heat flux) due to baroclinic instability (e.g., McIntyre and Weissman 1978; Thorncroft et al. 1993) and the associated vertical wave activity flux, thus it is a source for the wave activity. For a conservative flow (i.e. adiabatic and no wave dissipation), the eddy momentum flux convergence is solely balanced by the baroclinic eddy generation in steady state. The second term is the irreversible PV mixing, which is represented by the effective diffusivity, k_{eff}, multiplied by the Lagrangian background PV gradient $\partial Q/\partial Y$. This term manifests the role of the horizontal potential vorticity deformation, wave breaking and the resultant eddy dissipation at smaller scales, thus can be considered as a wave activity sink. The irreversible PV mixing can be caused by both linear dynamics (e.g., the critical latitude behavior (Chen and Held 2007), linear wave reflection (Lorenz 2014a,b) and changes in the index of refraction (Wu et al. 2013)) and nonlinear processes as the wave breaking (Thorncroft et al. 1993; Lu et al. 2013). When the eddy dissipation is strong, the wave activities resulting from the baroclinic growth are damped and thus cannot effectively contribute to the horizontal wave propagation in the upper troposphere and resultant eddy momentum flux. The third term denotes the negative time tendency of finite amplitude wave activity A, which is negligible in the long-term response to the imposed forcing. The final term $\Delta\Sigma$ denotes the diabatic source/sink of wave activity. Therefore, Eq. (4) provides a diagnostic framework to quantify the contributions of eddy growth and eddy dissipation to balance the eddy momentum flux convergence that drives the eddy-driven jet in response to the imposed thermal forcing. Note that the diagnostic does not necessarily claim that the eddy momentum flux convergence is caused by the eddy generation and dissipation. It provides a wave activity constraint between the eddy momentum flux convergence, eddy generation and eddy dissipation in equilibrium, which enables us to quantify their changes to the imposed thermal forcing. This is analogous to Earth's energy constraint between the meridional energy transport, incoming short wave radiation and outgoing long wave radiation (Hartmann 2015).

Accepted for publication in *Journal of the Atmospheric Sciences*. DOI 10.1175/JAS-D-21-0307.1

3. Sensitivities of the equilibrated responses

In this section, the equilibrated atmospheric responses to the imposed thermal forcing are depicted. Figure 2a tests the sensitivity of the surface zonal wind to the meridional displacement of the thermal forcing Δy in both UP and LOW runs. The zonal winds show a gradual poleward migration as the imposed upper-/lower-level thermal forcing is displaced more poleward. From the perspective of zonal momentum balance, the surface zonal wind is dominantly driven by the vertically averaged eddy momentum flux convergence. As depicted in Fig. 2b, the response of the eddy momentum flux convergence to the increase of the forcing displacement distance Δy exhibits a monotonic poleward shift. Meanwhile, the latitude of the vertically averaged maximum eddy kinetic energy as a function of Δy is also plotted in Fig. 2c. The EKE exhibits a monotonic poleward shift and weakened intensity to the imposed thermal forcing. Comparisons of the responses between the UP (solid lines) and LOW (dashed lines) runs further show that the shifts in zonal wind and eddy momentum forcing are both stronger in the UP runs, especially for the equatorward center of action, implying that upper-level thermal forcing is more efficient in displacing the eddy-driven jet.

Sensitivity of the atmospheric response to the vertical level of imposed thermal forcing is also examined in Figs. 2d-f. Both the zonal wind and the vertically averaged eddy momentum flux convergence display stronger poleward displacement as the vertical level of the imposed thermal forcing is raised. The robustness of the above sensitivity runs is also tested by repeating the above simulations but cutting the vertical extent of thermal forcing in half. The conclusions are all the same (results thus not shown). Therefore, all of our sensitivity experiments suggest that the upper-level thermal forcing is more efficient in shifting the eddy-driven jet.

4. Quantifying the eddy responses to the imposed thermal forcing

a. Diagnosing the eddy generation and dissipation responses through FAWA analysis

The possible reason for the higher efficiency of upper-level thermal forcing in displacing the eddy-driven jet is then explored. For simplicity, only the cases with latitudinal displacement $\Delta y = 1250$ km are displayed. Figure 3 compares the vertical structures of the equilibrated responses of the eddy fluxes between UP and LOW runs. The latitudinal dipolar response patterns of the eddy momentum flux convergence and eddy heat flux in both runs denote a poleward displacement, but

Accepted for publication in *Journal of the Atmospheric Sciences*. DOI 10.1175/JAS-D-21-0307.1

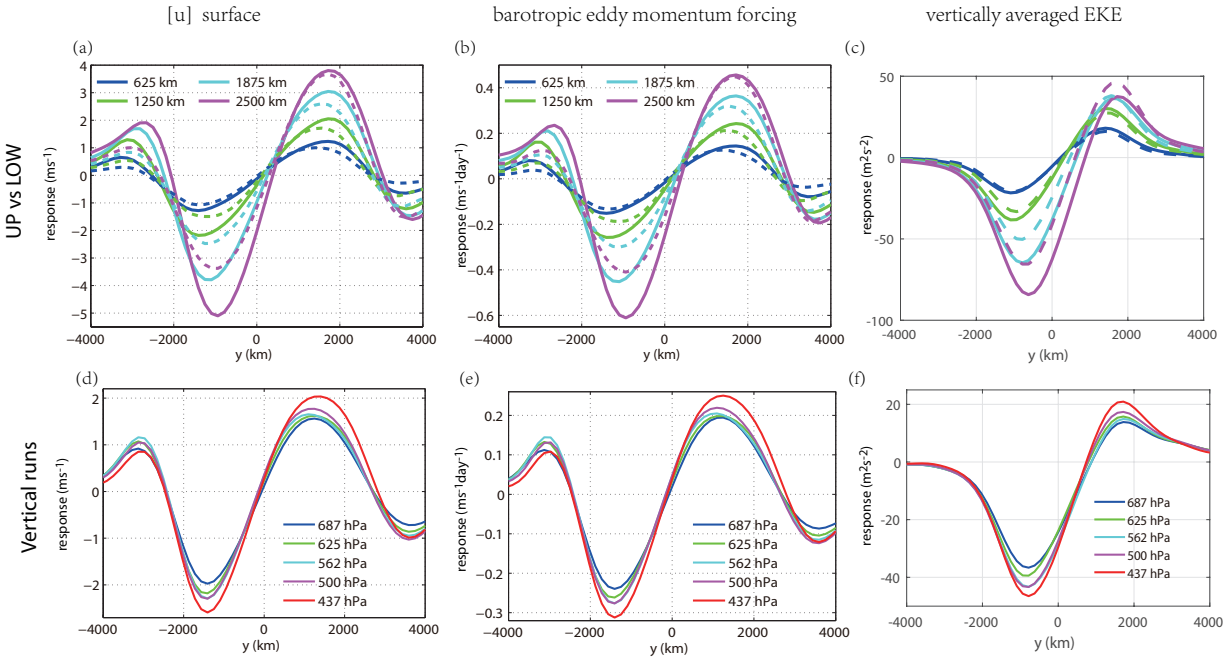

FIG. 2. Equilibrated response of the zonal-mean (a) surface zonal wind (unit: ms^{-1}), (b) vertically averaged eddy momentum flux convergence (unit: $ms^{-1}day^{-1}$) and (c) vertically averaged eddy kinetic energy (unit: m^2s^{-2}) in each UP and LOW runs. The solid (dashed) line denotes the response in the UP (LOW) runs. (d)-(f) same as (a)-(c), respectively, but for the Vertical runs.

the magnitude of the eddy response is stronger in the UP run. The stronger eddy responses in the UP run can be further elucidated by analyzing the FAWA budget in Eq.(4). The difference of Eq. (4) between the UP/LOW run and CTL run will show the responses of eddy momentum flux convergence, eddy generation, eddy dissipation and diabatic term. In the equilibrated state (Figs. 3c and d), though the responses of the eddy momentum flux convergence display a similar dipolar pattern, the relative contributions of eddy generation and eddy dissipation to such response are significantly different between UP and LOW runs. In the UP run, the baroclinic eddy generation shows a much stronger dipolar structure than the momentum flux convergence, which overwhelms the damping role of eddy dissipation in response to the upper-level thermal forcing. However, in the LOW run both the eddy generation and dissipation terms positively correlate to the poleward shift of the eddy momentum flux convergence, with the latter playing a more dominant role.

The response of eddy dissipation can be further decomposed into the part resulting from the change by effective diffusivity ($-\Delta k_{eff} \cdot \partial Q/\partial Y$) and the part resulting from the change of the

Accepted for publication in *Journal of the Atmospheric Sciences*. DOI 10.1175/JAS-D-21-0307.1.

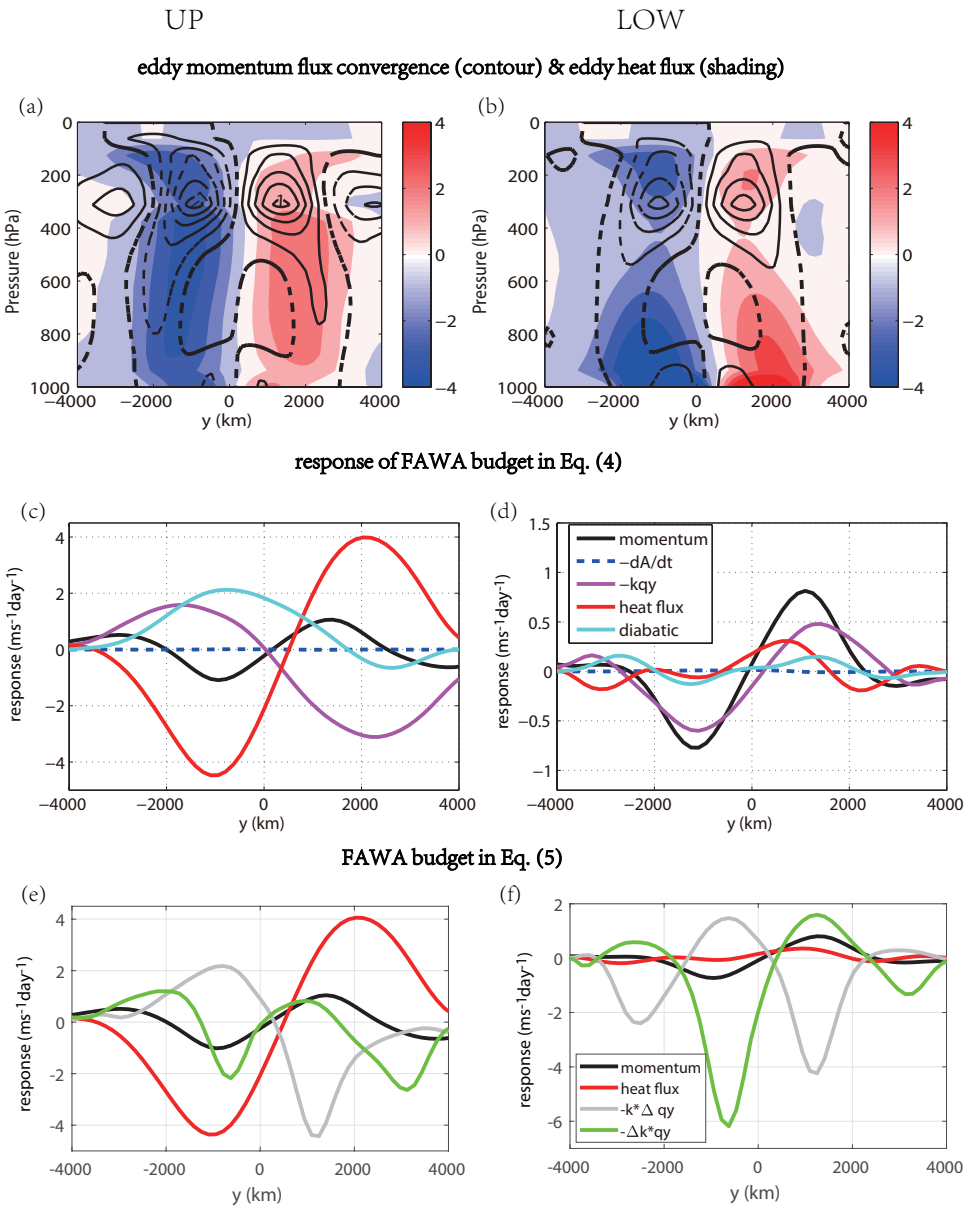

FIG. 3. Equilibrated response of the zonal-mean eddy momentum flux convergence (contour, int: 0.2 $ms^{-1}day^{-1}$) and eddy heat flux (shading, int: 1 Kms^{-1}) in the (a) UP and (b) LOW runs to the displacement of $\partial[T_e]/\partial y$ by 1250 km. (c)-(d) are the equilibrated response of each term (unit: $ms^{-1}day^{-1}$) in the FAWA budget of Eq. (4) at 312.5 hPa in the UP and LOW run, respectively. Note that the scale in panel (d) is smaller than that in panel (c). (e)-(f) are same as (c)-(d) but for the budget of Eq. (5).

background PV gradient ($-k_{eff} \cdot \Delta\partial Q/\partial Y$). Therefore, the eddy response to the diabatic heating is roughly in balance as follows in the equilibrium.

Accepted for publication in *Journal of the Atmospheric Sciences*. DOI 10.1175/JAS-D-21-0307.1

$$\Delta(-\frac{\partial[u^*v^*]}{\partial y}) \approx \underbrace{\Delta(-\frac{\partial}{\partial p}\frac{f[v^*\theta^*]}{\partial\theta_s/\partial p})}_{eddy\ generation} \underbrace{-\Delta(k_{eff})\frac{\partial Q}{\partial Y} - k_{eff}\Delta(\frac{\partial Q}{\partial Y})}_{eddy\ dissipation}. \quad (5)$$

Figures 3e-f compare the equilibrated response of each component in Eq. (5) between UP and LOW runs. In both two runs, the first two terms on the RHS of Eq. (5) act to enhance the latitudinal shift of the jet, while the last term acts as a damping. The primary difference between the UP and LOW runs lies in the relative importance of these three components. In the UP runs, the net effect of the last two terms is to damp the poleward shift of eddy momentum flux convergence, but this is offset by the strong and dominant contribution of the eddy generation. In the LOW run, the contribution of the eddy generation is very weak. The contribution due to the change of effective diffusivity becomes dominant, acting as the main process leading to the poleward shift of the jet.

The relative contributions of these three components to the jet shift are also compared in all the sensitivity experiments. As shown in Fig. 4a, the eddy generation term exhibits a much greater latitudinal shift in response to the upper-level thermal forcing, suggesting its primary role in the eddy response to upper-level forcing. In contrast, the effective diffusivity, as shown in Fig. 4b, is more sensitive to the lower level thermal forcing. The latitudinal displacement of k_{eff} in the UP run is much weaker than the shift of eddy momentum forcing, indicating that it only plays a secondary role in the eddy response. The background PV gradient in Fig. 4c shows similar trends of latitudinal shift in UP and LOW runs, with the trend in the UP runs slightly stronger. Similar comparisons are also conducted between the above three components and the latitudinal displacement of the eddy-driven jet. The jet latitude is obtained by estimating the location of the surface westerly maximum using an interpolation method. The results, as shown in Figs. 4d-f, are almost the same as in Figs. 4a-c. This again shows that the latitudinal shift of the eddy-driven jet can be well quantified by the change of the upper-level averaged eddy momentum flux convergence from the perspective of FAWA sensitivities. The above diagnostic analyses further suggest the importance of the eddy generation response in the UP runs and eddy dissipation response in the LOW runs.

Accepted for publication in *Journal of the Atmospheric Sciences*. DOI: 10.1175/JAS-D-21-0307.1

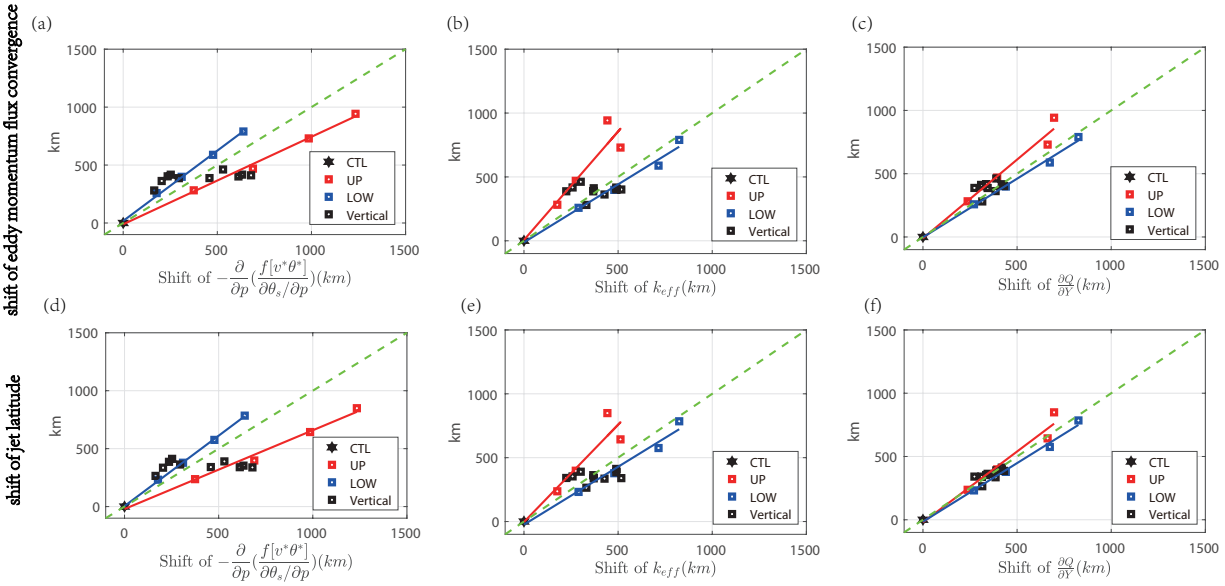

FIG. 4. Displacements of the peak latitudes of the upper-level averaged convergence of the eddy momentum flux against the latitudinal shift of (a) vertical differential of eddy heat flux $-\frac{\partial}{\partial p}\frac{f\,[v^*\theta^*]}{\partial\theta_s/\partial p}$, (b) effective diffusivity k_{eff} and (c) PV gradient $\partial Q/\partial Y$. (d)-(f) same as (a)-(c) but for the shifts of the eddy-driven jet. The solid red and blue lines denote the linear least square fit of the relation in UP and LOW runs, respectively. The green dashed line denotes the one-to-one line.

b. Quantifying the eddy generation response by overriding experiments

We next strive to quantify the eddy generation responses by carrying out overriding experiments similar to Nie et al. (2016) and Chen et al. (2020). Specifically, the *baroclinic generation run* is designed to keep the baroclinic eddy generation response active but suppress the eddy dissipation response associated with the barotropic winds. As introduced in detail in Nie et al. (2016), this is achieved by the fact that the response of eddy dissipation is mostly controlled by the variation of barotropic zonal wind $[u]_{bt}$, which is estimated as the vertical average of zonal mean zonal wind. In this experiment, thermal forcing is kept the same as in the sensitivity runs, but $[u]_{bt}$ in PV advection in the governing equation of the model is fixed as the climatological $[u]_{bt}$ in the CTL run. Then the impacts of the imposed thermal forcing on local baroclinic eddy generation are active, but the instantaneous barotropic zonal wind in the PV advection is unchanged and not allowed to affect the horizontal wave propagation, breaking and the resultant eddy mixing,

Accepted for publication in *Journal of the Atmospheric Sciences*. DOI 10.1175/JAS-D-21-0307.1

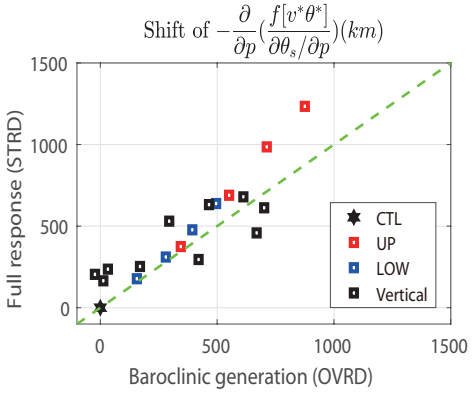

FIG. 5. Relationship of the vertical differential of eddy heat flux $-\frac{\partial}{\partial p}\frac{f[v^*\theta^*]}{\partial\theta_s/\partial p}$ between the standard runs and the corresponding baroclinic generation runs for all experiments. In the baroclinic generation run, the barotropic zonal wind in the PV advection is fixed thus the barotropic eddy feedback is eliminated but the baroclinic generation is retained. See more details in Appendix A.

and thus the eddy dissipation response is suppressed (also see Appendix A for details). Figure 5 displays the latitudinal displacement of the eddy generation term $-\frac{\partial}{\partial p}(\frac{f[v^*\theta^*]}{\partial\theta_s/\partial p})$ in all standard sensitivity runs versus the corresponding baroclinic generation runs. It is clear that the shift of eddy generation term in two sets of experiments mostly lies along the one-to-one line, suggesting that the eddy generation term in the overriding runs almost displaces the same latitude as that in the standard runs. Therefore, the eddy generation response in the standard runs can be well captured and reproduced by the overriding experiments which only keep the baroclinic generation of eddies in response to the forced temperature gradient.

The spatial pattern of the equilibrated eddy response in both standard runs and overriding runs is further compared by examining the E-P flux and eddy momentum flux convergence in Fig. 6. As a direct response to the poleward displacement of the upper-level temperature gradient, the E-P vector in the baroclinic generation run (Fig. 6b) shows pronounced upward (downward) wave activity flux on the poleward (equatorward) side. The upward wave activity flux peaks in the middle to upper troposphere, and then gives rise to a convergence of E-P flux in the upper troposphere but a divergence below (shadings), which matches well to the response pattern in the UP run shown in Fig. 6a thus again suggests the dominant role of baroclinic generation in the eddy response to the thermal forcing. Figures 6c-d display the responses in the LOW run and the corresponding overriding run. As a direct response to lower-level thermal forcing, the E-P vector of the baroclinic

Accepted for publication in *Journal of the Atmospheric Sciences*. DOI 10.1175/JAS-D-21-0307.1

generation run shown in Fig. 6d displays upward (downward) wave activity flux on the poleward (equatorward) side in the lower troposphere. Such a response pattern also matches well to the lower-tropospheric E-P vector pattern in the standard LOW run shown in Fig. 6c. The above E-P vector comparison illustrates that the spatial pattern of the E-P flux divergence or equivalently eddy PV flux can be well captured by the baroclinic eddy generation runs.

The eddy momentum flux response in the overriding runs (black contours in Fig. 6b) further suggests the different role of the baroclinic generation response in UP and LOW runs. The baroclinic generation run can reproduce almost 2/3 of the magnitude of eddy momentum flux response with a roughly similar pattern compared with that in the standard UP run in Fig. 6a. There is certain shift in the response center in the poleward-side latitude for the eddy momentum flux convergence, which is reasonable as the eddy response is fully nonlinear and there is coupling between the eddy generation, dissipation and eddy momentum flux. In contrast, the baroclinic eddy generation plays a negligible role for eddy momentum flux convergence in response to lower-level thermal forcing. The conclusion also holds for the response of the vertically-averaged eddy momentum flux convergence (results are similar thus not shown here). This implies that the response of the eddy momentum flux associated with the eddy generation may depend on the vertical structure of the thermal forcing.

in the standard runs. The baroclinic generation run can reproduce almost 2/3 of the magnitude of eddy momentum flux with a roughly similar pattern compared with that in the standard UP run. In contrast, the baroclinic eddy generation plays a negligible role in response to lower-level thermal forcing. The conclusion also holds for the response of the vertically-averaged eddy momentum flux convergence (figures not shown). This implies that the momentum contribution from the eddy generation may depend on the vertical structure of the thermal forcing.

Figure 7 examines the sensitivities of the equilibrated eddy responses to the vertical level of imposed thermal forcing in both standard Vertical runs and corresponding overriding runs. In the standard Vertical runs, as shown in Figs. 7a-c, as the imposed forcing is raised, the peak of vertical E-P vector is lifted and the strength of horizontal E-P vector in the upper-troposphere is enhanced, corresponding to stronger poleward displacement of the eddy momentum flux convergence (black contours). The overriding runs further show that the baroclinic response of eddies and its contribution to the momentum shift are very sensitive to the vertical level of thermal forcing. As shown

Accepted for publication in *Journal of the Atmospheric Sciences*. DOI 10.1175/JAS-D-21-0307.1

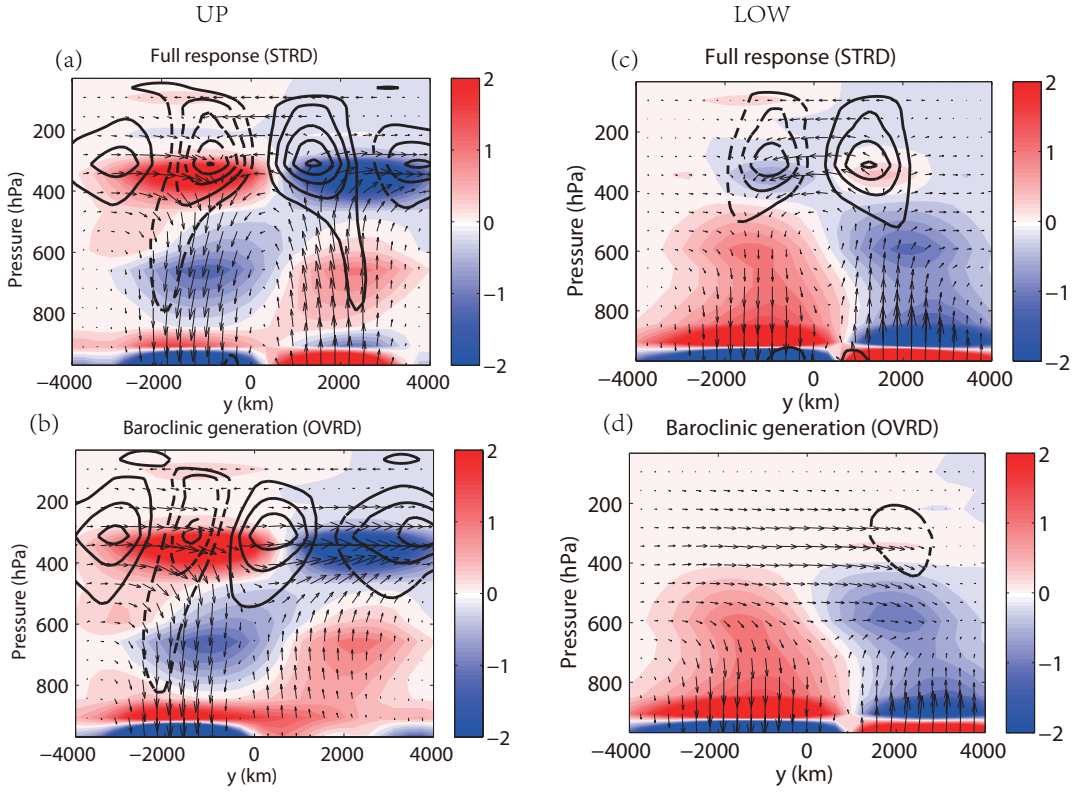

FIG. 6. Equilibrated responses of E-P flux (vector), E-P flux divergence (shading, int: $0.2\,ms^{-1}day^{-1}$) and eddy momentum flux convergence (black contour, int: $0.2\ ms^{-1}day^{-1}$) in the (a) UP run and (b) the corresponding baroclinic generation run, with $\partial[T_e]/\partial y$ displaced by 1250 km. In the baroclinic generation run, the barotropic zonal wind in the PV advection is fixed thus the barotropic eddy feedback is eliminated but the baroclinic generation is retained. See more details in Appendix A. (c)-(d) same as (a)-(b), respectively, but for the LOW run and its corresponding overriding run.

in Figs. 7d-f, in response to low level forcing (i.e. Fig. 7d), the anomalous eddies are mostly confined in the low levels, with very weak response in the eddy momentum flux in the upper level. As the vertical level of thermal forcing is lifted, the eddy momentum response aloft strengthens significantly. Thus, all of our overriding experiments demonstrate that eddy momentum response due to the change of baroclinic generation of eddies is sensitive to the vertical level of thermal forcing. Only the anomalous eddy generation that can vertically propagate into the upper troposphere can have a striking impact on the eddy momentum flux, which pushes the jet shift more efficiently and dominates the eddy response. The conclusion holds for all the experiments, independent of the width of imposed thermal forcing.

Accepted for publication in *Journal of the Atmospheric Sciences*. DOI 10.1175/JAS-D-21-0307.1.

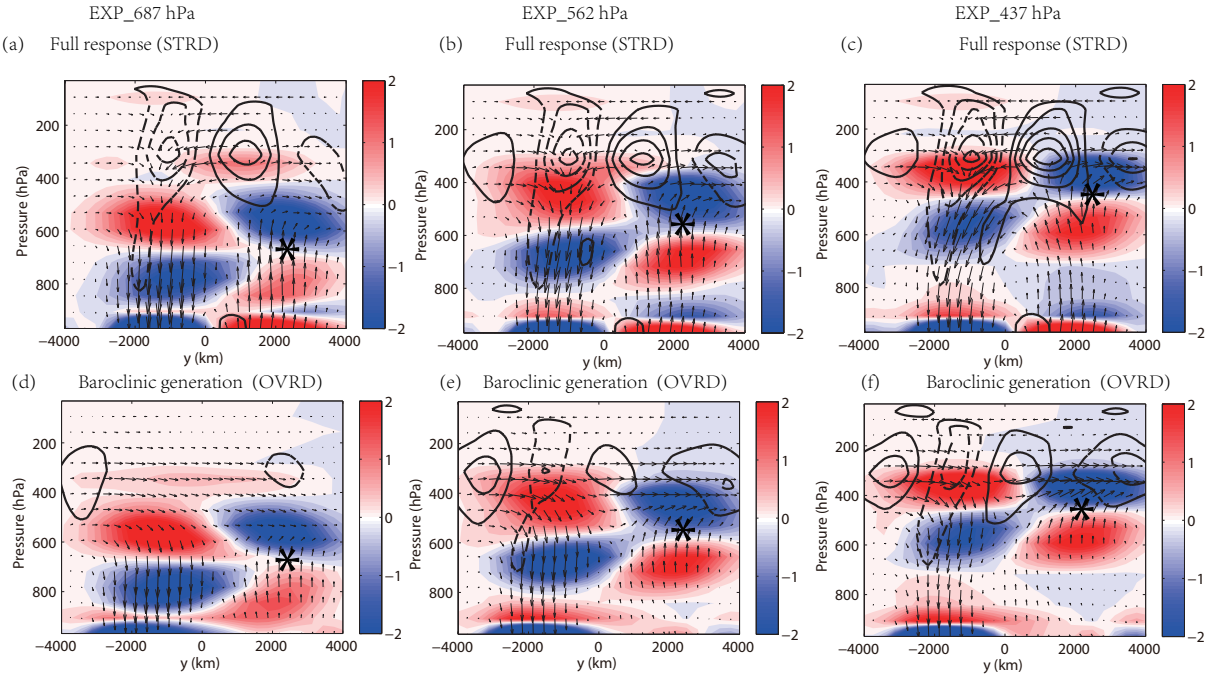

FIG. 7. Same as Fig.6 but for the Vertical runs with the central level of thermal forcing located at 687.5 hPa (left column), 562.5 hPa (middle column) and 437.5 hPa (right column). The black asterisk denotes the location where the imposed thermal forcing is largest.

The overriding experiment analyses suggest that the eddy generation response is linked to the change of forced temperature gradient. Given the above understanding, we next to quantify the eddy generation response based on the imposed temperature gradient $\partial T_e/\partial y$. As shown in Fig. 8a, the latitudinal change of eddy generation is relatively loosely-distributed, suggesting that it is not strongly proportional to the vertically averaged $\langle \partial T_e/\partial y \rangle$. This can be understood through examining the vertical profiles of the anomalous eddy heat flux over the stratification $-\frac{f[v^*\theta^*]}{\partial \theta_s/\partial p}$ in the sensitivity experiments. As shown in Figs. 7a-c, they exhibits evident vertical structure, all peaking around the level of imposed thermal forcing. For the lower level forcing, the anomalous eddy heat flux is confined in the lower troposphere, with negligible contribution to the eddy momentum flux in the upper troposphere. As the thermal forcing is lifted upward, the anomalous eddy heat flux exhibits stronger vertical differential in the upper troposphere, which, as in Eq. (4), denotes stronger contribution to the budget of the eddy momentum flux convergence. This also suggests that the eddy momentum flux response not only depends on meridional variations of thermal forcing

Accepted for publication in *Journal of the Atmospheric Sciences*. DOI 10.1175/JAS-D-21-0307.1

but also depends on the vertical variations of thermal forcing, as in the parameterization of eddy momentum flux in a 2D model (e.g. Stone and Yao 1987).

The above result suggests that the contribution of the eddy generation term should be more related to the thermal perturbation in the upper troposphere. Thus, we investigate the relationship between the eddy generation term and the upper-level averaged $\partial T_e/\partial y$ in Fig. 8b by examining all standard experiments in Fig. 8a. We find that the eddy generation term can be best estimated by the thermal perturbation averaged between 750 hPa and the top of the model, as shown in Fig. 8b, in which the eddy generation term in the UP runs exhibits a much stronger latitudinal shift with the stronger upper level averaged $\partial T_e/\partial y$ compared with the LOW runs and Vertical runs. Similar results are also found between the eddy generation term in the overriding runs and the target temperature gradient, as shown in Figs. 8c-d. Since the vertical sensitivity of the eddy response holds for all experiments and is independent of the width of thermal forcing, we further suggest that stronger dependence of the eddy generation term on the upper-level temperature gradient and the possible reason for the 750 hPa cutoff may bear a dynamical reason: the vertical profile of the critical layer. Eddies generated by baroclinic instability below the critical layer cannot propagate as waves and are dissipated in their source latitude (e.g., McIntyre and Weissman 1978; Lindzen and Barker 1985; Simmons and Hoskins 1978; Gliatto and Held 2020). Only the anomalous eddy generation near or above critical layer can radiate and propagate upward to the upper troposphere and then have a striking impact on the eddy momentum flux. The details are discussed in Appendix B.

c. Quantifying the eddy dissipation response through a multi-wavenumber theory

As suggested in the previous FAWA diagnostics, changes in eddy diffusivity make a leading contribution to the total eddy dissipation response while changes in background PV gradient play a secondary damping role. We next quantify the response of eddy diffusivity through a linear multi-wavenumber theory based on the information of EKE covariance spectrum and critical line distribution, which was firstly proposed by Chen et al. (2015) in oceanic eddy diffusivity analysis. Specifically, the eddy diffusivity centered at a fixed location y is

$$k_{eff}(y) = \frac{1}{2}\int_{-\infty}^{\infty} S_{EKE}(k', |\mathbf{U}|, y)dk', \tag{6}$$

Accepted for publication in *Journal of the Atmospheric Sciences*. DOI 10.1175/JAS-D-21-0307.1

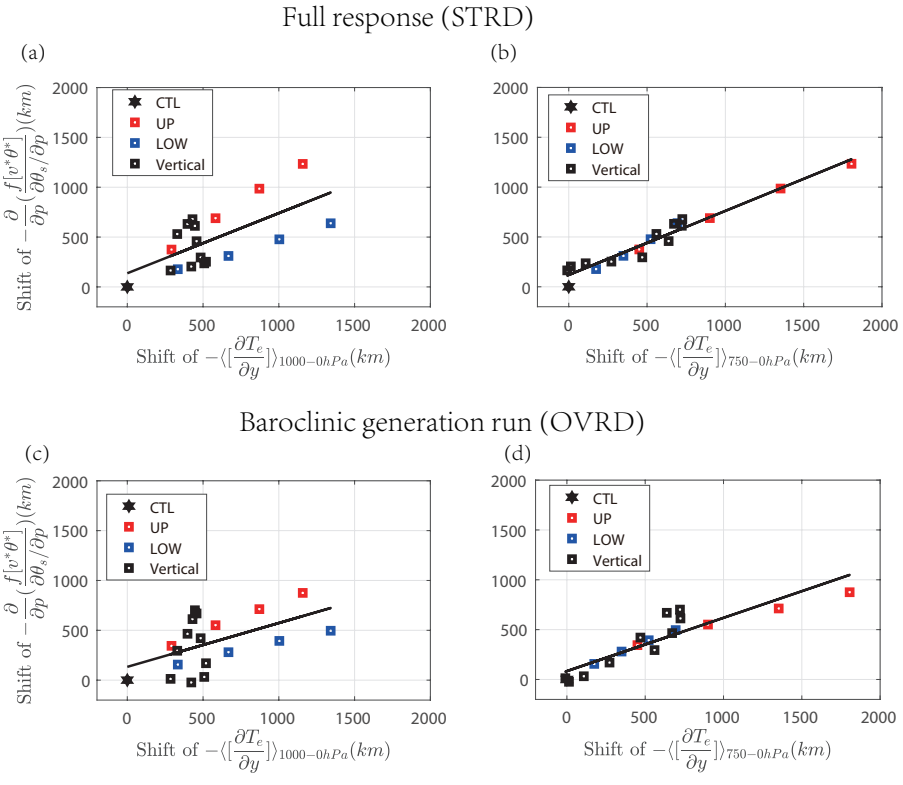

FIG. 8. (a) Displacements of the peak latitudes of the vertical differential of eddy heat flux $-\frac{\partial}{\partial p}\frac{f[v^*\theta^*]}{\partial\theta_s/\partial p}$ in the standard experiments against the latitudinal shift of the vertical mean $\partial[T_e]/\partial y$. (b) same as (a) but for the sensitivity to $\partial[T_e]/\partial y$ averaged over 750 hPa to the top of the model. (c)-(d) are same as (a)-(b) but for the sensitivities in the overriding baroclinic generation experiments. The solid line in panel (a)-(d) denotes the linear least square fit of the relationship.

where k is the zonal wave number, and $S_{EKE}(k', c, y)$ is the two-dimensional spectrum of the EKE along the slice where the zonal wind U equals to phase speed c. More details of the method can be found in Chen et al. (2015). Figure 9a shows the profile of the zonal wind U and the total co-spectra of EKE as a function of latitude and phase speed. The EKE co-spectra peaks at the jet center and decreases towards the jet flanks. Figure 9b further displays the spatial profile of the estimated diffusivity according to Eq. (6). The eddy diffusivity is strongest around the critical line region at the jet flanks and weakest at the jet center, which is consistent with the eddy diffusivity estimated through the residual of FAWA budget. To further test the effectiveness of multi-wavenumber theory in estimating the eddy diffusivity, Fig. 9c compares the shift of eddy diffusivity estimated by multi-wavenumber theory and that derived from the FAWA budget residual. It is clear that

Accepted for publication in *Journal of the Atmospheric Sciences*. DOI 10.1175/JAS-D-21-0307.1.

the displacement of the two estimated diffusivities is closely along the one-to-one line, although the multi-wavenumber estimate is slightly weaker. This implies that the multi-wavenumber theory can reasonably capture a large portion of the shift of the eddy diffusivity, but still a small portion resulting from nonlinearities cannot be resolved by this theory.

The relative roles of EKE covariance spectrum and critical line in shifting the eddy diffusivity is further examined by decomposing the standard eddy diffusivity estimated through the multi-wavenumber theory into the part resulting from the change of EKE spectrum (EKE-perturbed diffusivity) and the part resulting from the change of zonal wind (U-perturbed diffusivity). Specifically, the EKE-perturbed diffusivity is estimated following Eq. (6) but using the EKE cospectrum from the UP/LOW/Vertical runs and the zonal wind from the CTL run. In contrast, the U-perturbed diffusivity is derived using the EKE cospectrum from the CTL run and the zonal wind from the UP/LOW/Vertical runs. Figure 10 compares the latitudinal displacement of the standard eddy diffusivity versus the latitudinal displacement of the EKE-perturbed diffusivity and U-perturbed diffusivity. As shown in Fig. 10a, the EKE-perturbed diffusivity exhibits small displacement compared to the standard diffusivity, implying that perturbation in EKE cospectrum plays minor role in shifting the eddy diffusivity. In contrast, as shown in Fig. 10b, the U-perturbed diffusivity is displaced poleward significantly and exhibits one-to-one relation to the shift of standard diffusivity. This implies that the shift of effective diffusivity is mostly governed by the change of the zonal wind.

Figures 11a,b further test the sensitivities of the latitudinal displacement of the estimated eddy diffusivity to the displacement of the barotropic zonal wind in the standard experiments. For both eddy diffusivities estimated by multi-wavenumber theory and FAWA budget, they show clear linear relation to the barotropic zonal wind, which again confirms the important role of the shift of the barotropic zonal wind and resultant critical line in governing the response of the eddy dissipation as in previous studies (Nie et al. 2014, 2016). We further quantify the latitudinal shift of the eddy diffusivity based on the imposed forcing. Figures 11c,d test the sensitivities of the estimated diffusivity to the displacement of zonally-symmetric barotropic zonal wind $< U_e >$. Here U_e is calculated as the zonal wind from the zonally symmetric version of our QG model. In our model calculation, the surface thermal wind is set to zero. For all the sensitivity experiments and diffusivity estimation methods, the change of k_{eff} can be well estimated by the change of

Accepted for publication in *Journal of the Atmospheric Sciences*. DOI 10.1175/JAS-D-21-0307.1

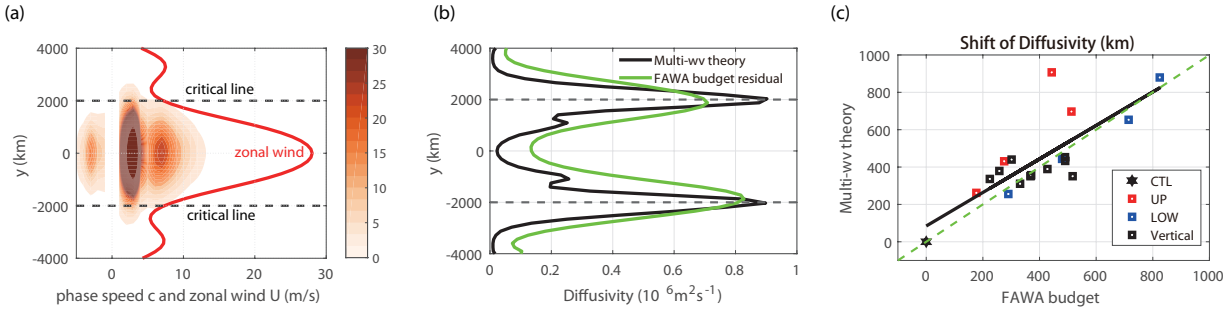

FIG. 9. (a) Co-spectra of 312.5 hPa EKE as a function of zonal phase speed and latitude for standard CTL run. The red solid line denotes the zonally averaged zonal wind at 312.5 hPa. The gray dashed lines denote the location of critical line where the zonal wind is equal to the phase speed. (b) Profile of the 312.5 hPa estimated eddy diffusivity based on the multi-wavenumber theory in Eq. (6) and that based on the FAWA budget in Eq. (4). The gray dashed lines denote the location of critical line. (c) Displacement of the peak latitude of the estimated maximum eddy diffusivity based on the multi-wavenumber theory versus the latitudinal shift of the maximum eddy diffusivity estimated based on the FAWA budget in Eq. (4). The dashed green line denotes the one-to-one line. The black solid line denotes the linear fit between the two estimated diffusivities.

$< U_e >$, no matter the vertical level of the thermal forcing imposed. Since U_e is the thermal wind of $\partial T_e/\partial y$, the above results imply that the eddy dissipation response can be quantified based on the imposed vertically-averaged thermal wind $< U_e >$. These results have important implication for the eddy diffusivity prediction. If the EKE spectrum of an unforced system is known and then a zonal wind shift is artificially added, the final location of the diffusivity can be thus derived based on the imposed zonal wind change. This suggests a feedback mechanism by which the shift in barotropic zonal wind may organize the eddy diffusivity of PV mixing.

5. Summary and Discussion

Using a nonlinear β plane multi-level QG channel model, this study investigates the latitudinal shift of the eddy-driven jet in response to upper- and lower-level thermal forcing. Our sensitivity experiments show that the latitudinal position of the eddy-driven jet is more sensitive to the upper-

Accepted for publication in *Journal of the Atmospheric Sciences*. DOI 10.1175/JAS-D-21-0307.1.

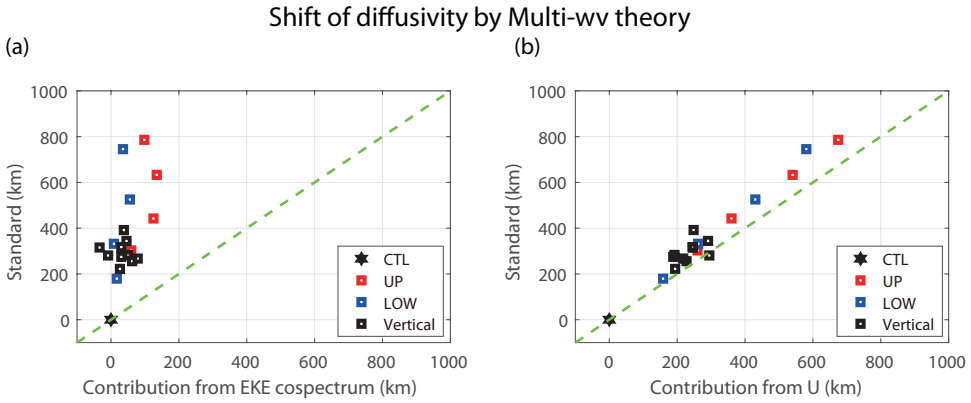

FIG. 10. Relative contribution of EKE covariance spectrum and zonal wind changes in displacing the eddy diffusivity using the multi-wavenumber theory. (a) Latitudinal displacement of the peak latitude of 500-125 hPa averaged standard eddy diffusivity versus the latitudinal shift of EKE-perturbed diffusivity. (b) same as (a) but for the standard diffusivity shift versus the U-perturbed diffusivity shift. The EKE-perturbed/U-perturbed diffusivity is derived using the multi-wavenumber theory estimation but with only EKE cospectrum/zonal wind varied but the zonal wind/EKE spectrum fixed to that of CTL run. The dashed green line denotes the one-to-one line.

level thermal forcing compared to the lower-level forcing. This finding is consistent with the model studies of Yuval and Kaspi (2016, 2017). Our FAWA diagnostics show that the dominance of the upper-level thermal forcing over the lower-level thermal forcing can be understood from their different influence on eddy generation and dissipation responses that affect the jet shift. The upper-level thermal forcing is more efficient in shifting the eddy-driven jet via its dominant influence on the eddy generation (summarized in the schematic diagram of Fig. 12).

Based on the above understanding, we further quantify the eddy response, including both the response in eddy generation and eddy dissipation, and relate them to the upper/lower level thermal forcing. This is helpful for predicting the eddy-driven jet shift in response to the thermal forcing. Our study shows that the eddy generation response is sensitive to the vertical level of the imposed forcing and can be quantified by the temperature gradient in the upper troposphere. This helps explain why previous studies (Rivière 2011; Yuval and Kaspi 2016) were successful in explaining the jet shift from the perspective of linear baroclinic instability. Different from the scenario proposed in Rivière (2011), in which long waves become more unstable in response to the enhanced upper-level temperature gradient thus more anticyclonic wave breaking occurs acting to push the

Accepted for publication in *Journal of the Atmospheric Sciences*. DOI 10.1175/JAS-D-21-0307.1.

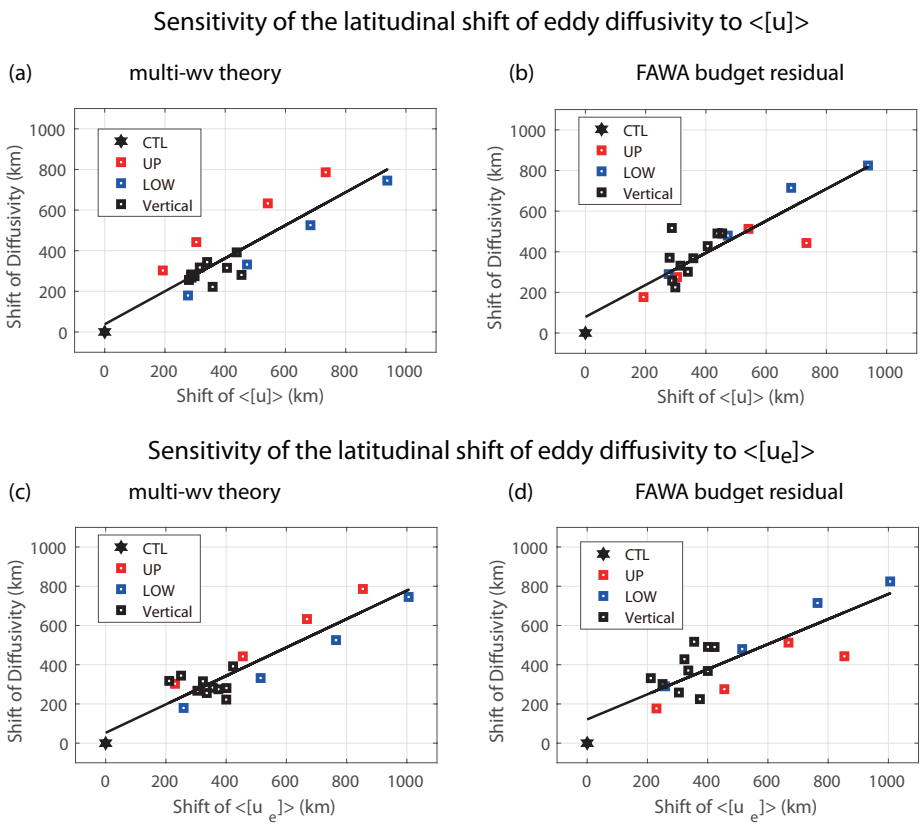

FIG. 11. (a) Sensitivity of the latitudinal displacement distance of 500-125 hPa averaged eddy diffusivity from multi-wavenumber theory in all experiments to the barotropic zonal wind in the same standard run. (b) Same as (a) but for the diffusivity derived from the FAWA budget in Eq. (4). (c),(d) are same as (a),(b) but for the sensitivity to the zonally-symmetric barotropic zonal wind.

jet poleward, the length scales of eddies in our study are almost unchanged with the imposed thermal forcing (results not shown). And unlike the global circulation model experiment in Yuval and Kaspi (2016), who explained stronger sensitivity of eddy activity to upper-level forcing by stronger background Eady growth rate there, in our experiment, the intensity of the background Eady growth rate is almost unchanged, and the stronger upper-level sensitivity is mostly because of stronger response of eddy heat flux which can vertically propagate into the upper levels.

In this study, we further quantify the eddy dissipation response through a multi-wavenumber theory based on the information of both EKE spectrum and critical line distributions. Our results suggest that the eddy dissipation response is mostly controlled by the variation of the imposed vertically-averaged thermal wind, no matter the vertical level of thermal forcing imposed. This

Accepted for publication in *Journal of the Atmospheric Sciences*. DOI 10.1175/JAS-D-21-0307.1.

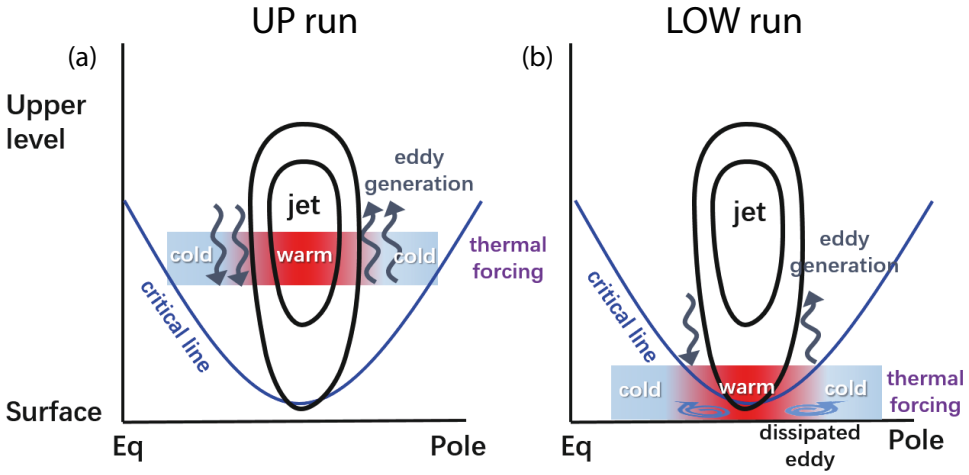

FIG. 12. Schematic for the different response of eddy generation to (a) upper-level and (b) lower-level thermal forcing. The black contours denote the climatological eddy-driven jet and the blue lines denote the distribution of critical line. The shadings denote the imposed thermal forcing, and the gray vertical arrows denote the anomalous vertical wave activity flux. The blue circular arrows in panel (b) denote the dissipated eddies below the critical layer. The response of eddy generation is sensitive to the vertical profile of the thermal forcing. Only the anomalous eddy generation near or above critical layer can radiate and propagate upward to the upper troposphere and affect the jet. The anomalous eddies generated below the critical layer cannot propagate as waves and are dissipated locally.

supports the relationship between the eddy dissipation and mean thermal wind in Novak et al. (2018). The insensitivity of eddy dissipation response to vertical level also helps us to understand why the vertical dependence of eddy-driven circulation is mainly caused by the vertical dependence of the eddy generation response.

Relating the eddy response to the imposed forcing is a fundamental issue in understanding the extra-tropical climate variability. Though theories relating eddy activity to background state and thermal forcing have been proposed such as the baroclinic adjustment (Stone 1978; Zurita-Gotor and Lindzen 2007; Zurita-Gotor 2007; Zurita-Gotor and Vallis 2009) and scaling theories (Green 1970; Stone 1972; Held 1978; Held and Larichev 1996; Schneider and Walker 2008; Zurita-Gotor and Vallis 2010) which relate an eddy field to its energy source, or the formalism of finite-amplitude wave-mean flow interaction (Nakamura and Zhu 2010; Nakamura and Solomon 2011), those theories are all based on a vertically uniform background state and thermal forcing. Our

Accepted for publication in *Journal of the Atmospheric Sciences*. DOI 10.1175/JAS-D-21-0307.1.

quantitative analysis extends this topic to the vertically non-uniform forcing by taking into account both the eddy generation as in Yuval and Kaspi (2017) and Mbengue and Schneider (2017), and the eddy dissipation as in Wang and Nakamura (2015) and Wang and Lee (2016). The quantitative relationship might be also helpful to understand and quantify the different impacts of lower-level thermal forcing associated with mid-latitude SST-fronts and upper-level thermal forcing due to latent heat release on the variability of eddy-driven jet (Hoskins and Valdes 1990; Hotta and Nakamura 2011).

It is important to note that, in this study, the eddy response to thermal forcing was investigated using a quasi-geostrophic channel model which does not consider the influence of spherical geometry and subtropical jet on the response of eddy driven jet. With the spherical effect, the eddy momentum flux in the real atmosphere has a clear asymmetry with a tendency toward more poleward than equatorward momentum flux. With the existence of a subtropical jet, the eddy generation could be more sensitive to the latitude of thermal forcing, with distinct eddy response for the thermal forcing imposed close to or far from the latitude of subtropical jet (e.g. Brayshaw et al. 2008). These effects may have significant influence on the shift of eddy generation and eddy-driven jet, which deserves further investigation in the future using a spherical primitive equation model.

We also want to point out that, with the aid of the FAWA framework, the relative contributions of eddy generation and eddy dissipation in the jet response can be explicitly diagnosed and quantitatively compared, however, this does not necessarily claim that the response of the eddy momentum flux convergence is caused by the changes in eddy generation and eddy dissipation. Our wave activity budget equation essentially provides a physical constraint between the three processes. This is analogous to the use of the top-of-atmosphere net radiative balance to understand atmospheric energy transport (assuming zero ocean transport). The net radiative balance may not directly cause atmospheric motion, but the energy transport must reach an energy balance with the energy source and sink in the equilibrium. More works are needed to further delineate the causality between the responses of eddy generation, eddy dissipation and eddy momentum flux to thermal forcing.

Accepted for publication in *Journal of the Atmospheric Sciences*. DOI 10.1175/JAS-D-21-0307.1

Acknowledgments. We are grateful to editor Anne Smith and two anonymous reviewers, whose comments and suggestions have greatly improved the quality of the manuscript. This study was supported by the National Key Research and Development Program under Grant 2022YFE0106900 and the NSF of China under grants 42175075. G.C. is supported by U.S. National Science Foundation grants AGS-1742178 and AGS-1832842.

Data availability statement. The quasi-geostrophic channel model data that support the findings of this study are available from the corresponding author upon reasonable request.

APPENDIX A

Design of the overriding experiments

To further quantify the baroclinic eddy feedbacks in the full response, an overriding technique is used to isolate the effect of barotropic advecting flow on PV mixing. The overriding technique is motivated by the fact that, as shown in Hartmann and Zuercher (1998), the barotropic zonal flow slightly influences the baroclinic energy conversion but evidently affects the barotropic decay process in an eddy life cycle. Thus, overriding the barotropic zonal flow mainly impacts the effective diffusivity by modulating potential vorticity advection.

More specifically, the governing equation in the model is the potential vorticity tendency equation:

$$\frac{\partial q}{\partial t} = \mathbf{V} \cdot \nabla_h q + \text{forcing terms}, \tag{A1}$$

where q is the potential vorticity. If we decompose each variable into the zonal average and the eddy components and assume the zonal mean meridional velocity [v] is small, the PV advection term in Eq.(A1) can be rewritten as

$$\mathbf{V} \cdot \nabla_h q = [u] \frac{\partial q^*}{\partial x} + v^* \frac{\partial [q]}{\partial y} + \mathbf{V}^* \cdot \nabla_h q^* \tag{A2}$$

where * denotes the eddy component and [ ] denotes zonal average. The first term on the right-hand-side of the equation just represents the PV advection by the zonal-mean zonal wind. The zonal-mean zonal wind can be further decomposed into the barotropic component of the zonal wind $[u]_{bt}$, which is estimated as the vertical average of the zonal wind, and the baroclinic component

Accepted for publication in *Journal of the Atmospheric Sciences*. DOI 10.1175/JAS-D-21-0307.1

of the zonal wind $[u]_{bc}$, which is defined as $[u]_{bc} = [u] - [u]_{bt}$. Thus, this term can be further decomposed as

$$[u]\frac{\partial q^*}{\partial x} = ([u]_{bt} + [u]_{bc})\frac{\partial q^*}{\partial x}. \tag{A3}$$

In the overriding experiment, we specify the barotropic zonal-mean zonal wind $[u]_{bt}$ in the PV advection and leave all the other terms, e.g. baroclinic zonal wind in the PV advection, and all the other fields such as wind, temperature and wave activity determined by the model evolution. As such, the overriding technique decouples the barotropic PV advection from baroclinic energy production. By doing so, we aim to suppress the barotropic eddy feedback associated with the change in barotropic zonal wind, but to keep the baroclinic eddy feedback associated with the change in meridional temperature advection and baroclinic zonal wind.

APPENDIX B

Vertical profile of the critical latitude

One possible reason for the contrasting response of the vertical wave activity flux to the upper- and lower-level thermal forcing might relate to the distribution of the critical level which by definition is the level where zonal wind U is equal to the phase speed C_r. As suggested by previous theoretical studies, the propagation of Rossby waves is determined by the background PV gradient and the distribution of critical line (e.g., Gliatto and Held 2020). The waves can freely propagate in the region where the zonal wind is larger than phase speed. If the baroclinic eddies are generated more vigorously in the lower troposphere where the zonal wind is less than phase speed, then the baroclinic waves could not propagate as waves and are dissipated in their source latitude. The phase speeds of the dominant waves are calculated following Gall (1976):

$$C_r = [k(\phi_s^2 + \phi_c^2)]^{-1}(\phi_c\frac{\partial \phi_s}{\partial t} - \phi_s\frac{\partial \phi_c}{\partial t}), \tag{B1}$$

where k is the zonal wavenumber, ϕ_s and ϕ_c are the real and imaginary parts of the Fourier coefficients of the stream function. Fig.B1 shows the critical lines of the dominant waves, which are wave-number 4-6 in these experiments, for each sensitive experiment. In the CTL run, the critical line is symmetric about the channel center, with highest critical level below 700 hPa at $|y| < 1500$ km. In the LOW run and $EXP_{687.5hPa}$ run, the critical line on the poleward side

Accepted for publication in *Journal of the Atmospheric Sciences*. DOI 10.1175/JAS-D-21-0307.1

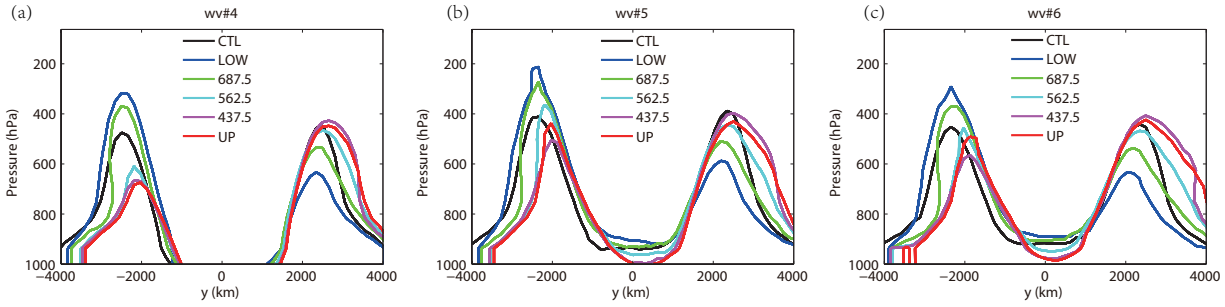

FIG. B1. The vertical profiles of the critical line (where the zonal wind equals to the phase speed) for dominant wave number (a) 4, (b), 5 and (c) 6 in different sensitivity runs.

is much lower. Anomalous baroclinic eddies generated on the poleward side cannot propagate as waves and are dissipated locally, thus exerting little effects on the upper-tropospheric wave propagation and eddy momentum flux. The distribution of the critical layer might also provide a possible explanation of that eddy generation term is linearly related to $\partial T_e/\partial y$ above 750 hPa. At y=1875 km in all experiments where the eddy growth is largest in this latitude, the steering level is almost 750 hPa. The 750 hPa critical layer does not allow the baroclinic eddies below this layer to propagate as waves, thus the wave activity flux that can vertically propagate upward is much less in response to the lower-level thermal forcing. Therefore, the baroclinic eddy generation term is more sensitive to the thermal forcing above this level.

References

Barnes, E. A., and D. W. J. Thompson, 2014: Comparing the roles of barotropic versus baroclinic feedbacks in the atmosphere's response to mechanical forcing. *J. Atmos. Sci.*, **71**, 177–194.

Brayshaw, D. J., B. Hoskins, and M. Blackburn, 2008: The Storm-Track Response to Idealized SST Perturbations in an Aquaplanet GCM. *J. Atmos. Sci.*, **65**, 2842–2860.

Burrows, D. A., G. Chen, and L. Sun, 2017: Barotropic and Baroclinic Eddy Feedbacks in the Mid-latitude Jet Variability and Responses to Climate Change-Like Thermal Forcings. *J. Atmos. Sci.*, **74**, 111–132.

Butler, A. H., D. W. Thompson, and R. Heikes, 2010: The steady-state atmospheric circulation response to climate change-like thermal forcings in a simple general circulation model. *J. Climate.*, **23**, 3474–3496.

Accepted for publication in *Journal of the Atmospheric Sciences*. DOI 10.1175/JAS-D-21-0307.1

Butler, A. H., D. W. J. Thompson, and T. Birner, 2011: Isentropic slopes, downgradient eddy fluxes, and the extratropical atmospheric circulation response to tropical tropospheric heating. *J. Atmos. Sci.*, **68**, 2292–2305.

Chang, E. K., 1998: Poleward-propagating angular momentum perturbations induced by zonally symmetric heat sources in the tropics. *J. Atmos. Sci.*, **55 (12)**, 2229–2248.

Chang, E. K. M., Y. Guo, and X. Xia, 2012: CMIP5 multimodel ensemble projection of storm track change under global warming. *J. Geophys. Res. - Atmos.*, **117 (D23)**, n/a–n/a.

Chen, G., and I. Held, 2007: Phase speed spectra and the recent poleward shift of Southern Hemisphere surface westerlies. *Geophys. Res. Lett.*, **34**, L21805, https://doi.org/10.1029/2007GL031200.

Chen, G., J. Lu, and L. Sun, 2013: Delineating the eddy-zonal flow interaction in the atmospheric circulation response to climate forcing: uniform SST warming in an idealized aqua-planet model. *J. Atmos. Sci.*, **70**, 2214–2233.

Chen, G., P. Zhang, and J. Lu, 2020: Sensitivity of the latitude of the westerly jet stream to climate forcing. *Geophys. Res. Lett.*, **47 (4)**, e2019GL086 563.

Chen, R., S. T. Gille, J. L. McClean, G. R. Flierl, and A. Griesel, 2015: A Multiwavenumber Theory for Eddy Diffusivities and Its Application to the Southeast Pacific (DIMES) Region. *J. Phys. Oceanogr.*, **45**, 1877–1896.

Deser, C., R. A.Tomas, and L. Sun, 2016: The role of ocean heat transport in the global climate response to projected arctic sea ice loss. *J. Climate.*, **29**, 6841–6859.

Deser, C., R.A.Tomas, and L. Sun, 2015: The Role of Ocean-Atmosphere Coupling in the Zonal-Mean Atmospheric Response to Arctic Sea Ice Loss. *J. Climate.*, **28**, 2168–2186.

Gall, R., 1976: A comparison of linear baroclinic instability theory with the eddy statistics of a general circulation model. *J. Atmos. Sci.*, **33**, 349–373.

Gliatto, M. T., and I. M. Held, 2020: Overtransmission of rossby waves at a lower-layer critical latitude in the two-layer model. *J. Atmos. Sci.*, **77 (3)**, 859–870.

Accepted for publication in *Journal of the Atmospheric Sciences*. DOI 10.1175/JAS-D-21-0307.1

Green, J., 1970: Transfer properties of the large-scale eddies and the general circulation of the atmosphere. *Quart. J. Roy. Meteor. Soc.*, **96**, 157–185.

Hartmann, D. L., 2015: *Global Physical Climatology: Second Edition*. 1-485 pp.

Hartmann, D. L., and P. Zuercher, 1998: Response of baroclinic life cycles to barotropic shear. *J. Atmos. Sci.*, **55**, 297–313.

Harvey, B. J., L. C. Shaffrey, and T. J. Woollings, 2014: Equator-to-pole temperature differences and the extra-tropical storm track responses of the CMIP5 climate models. *Clim. Dyn.*, **43**, 1171–1182.

Held, I., 1978: The vertical scale of an unstable baroclinic wave and its importance for eddy heat flux parameterizations. *J. Atmos. Sci.*, **35**, 572–576.

Held, I., and V. Larichev, 1996: A scaling theory for horizontally homogeneous, baroclinically unstable flow on a beta plane. *J. Atmos. Sci.*, **53**, 946–952.

Held, I., and E. O'Brien, 1992: Quasigeostrophic turbulence in a three-layer model: Effects of vertical structure in the mean shear. *J. Atmos. Sci.*, **49**, 1861–1870.

Hoskins, B. J., and P. J. Valdes, 1990: On the Existence of Storm-Tracks. *J. Atmos. Sci.*, **47**, 1854–1864.

Hotta, D., and H. Nakamura, 2011: On the Significance of the Sensible Heat Supply from the Ocean in the Maintenance of the Mean Baroclinicity along Storm Tracks. *J. Climate.*, **24**, 3377–3401.

Kidston, J., G. Vallis, S. Dean, and J. Renwick, 2011: Can the increase in the eddy length scale under global warming cause the poleward shift of the jet streams? *J. Climate.*, **24**, 3764–3780.

Kug, J.-S., and F.-F. Jin, 2009: Left-hand rule for synoptic eddy feedback on low-frequency flow. *Geophys. Res. Lett.*, **36**, L05709, https://doi.org/10.1029/2008GL036435.

Li, Y., D. W. J. Thompson, S. Bony, and T. M. Merlis, 2019: Thermodynamic control on the poleward shift of the extratropical jet in climate change simulations: The role of rising high clouds and their radiative effects. *J. Climate.*, **32 (3)**, 917 – 934, https://doi.org/10.1175/JCLI-D-18-0417.1.

Lindzen, R. S., and J. W. Barker, 1985: Instability and wave over-reflection in stably stratified shear flow. *J. Fluid Mech.*, **151**, 189–217.

Accepted for publication in *Journal of the Atmospheric Sciences*. DOI: 10.1175/JAS-D-21-0307.1

Lorenz, D., and E. DeWeaver, 2007: Tropopause height and zonal wind response to global warming in the IPCC scenario integrations. *J. Geophys. Res.*, **112**, 10119.

Lorenz, D., and D. Hartmann, 2003: Eddy-zonal flow feedback in the Northern Hemisphere winter. *J. Climate.*, **16 (8)**, 1212–1227.

Lorenz, D. J., 2014a: Understanding midlatitude jet variability and change using rossby wave chromatography: Methodology. *J. Atmos. Sci.*, **72**, 369–388.

Lorenz, D. J., 2014b: Understanding midlatitude jet variability and change using rossby wave chromatography: Poleward-shifted jets in response to external forcing. *J. Atmos. Sci.*, **71**, 2370–2389.

Lorenz, D. J., and D. L. Hartmann, 2001: Eddy-zonal flow feedback in the Southern Hemisphere. *J. Atmos. Sci.*, **58**, 3312–3327.

Lu, J., G. Chen, and D. M. Frierson, 2008: Response of the zonal mean atmospheric circulation to el nino versus global warming. *J. Climate.*, **21**, 5835–5851.

Lu, J., L. Sun, Y. Wu, and G. Chen, 2013: The role of subtropical irreversible PV mixing in the zonal mean circulation response to global warming-like thermal forcing. *J. Climate.*, **27**, 2297–2316.

Mbengue, C., and T. Schneider, 2017: Storm-track shifts under climate change: Toward a mechanistic understanding using baroclinic mean available potential energy. *J. Atmos. Sci.*, **74**, 93–110.

McIntyre, M. E., and M. A. Weissman, 1978: On Radiating Instabilities and Resonant Overreflection. *J. Atmos. Sci.*, **35 (7)**, 1190 – 1196.

Nakamura, N., and A. Solomon, 2010: Finite-amplitude wave activity and mean flow adjustments in the atmospheric general circulation. Part I: Quasigeostrophic theory and analysis. *J. Atmos. Sci.*, **67**, 3967–3983.

Nakamura, N., and A. Solomon, 2011: Finite-Amplitude Wave Activity and Mean Flow Adjustments in the Atmospheric General Circulation. Part II: Analysis in the Isentropic Coordinate. *J. Atmos. Sci.*, **68**, 2783–2799.

Accepted for publication in *Journal of the Atmospheric Sciences*. DOI 10.1175/JAS-D-21-0307.1

Nakamura, N., and D. Zhu, 2010: Finite-amplitude wave activity and diffusive flux of potential vorticity in eddy-mean flow interaction. *J. Atmos. Sci.*, **67**, 2701–2716.

Nie, Y., Y. Zhang, G. Chen, and X.-Q. Yang, 2016: Delineating the Barotropic and Baroclinic Mechanisms in the Midlatitude Eddy-Driven Jet Response to Lower-Tropospheric Thermal Forcing. *J. Atmos. Sci.*, **73**, 429–448.

Nie, Y., Y. Zhang, G. Chen, X.-Q. Yang, and D. A. Burrows, 2014: Quantifying Barotropic and Baroclinic Eddy Feedbacks in the Persistence of the Southern Annular Mode. *Geophys. Res. Lett.*, 8636–8644, https://doi.org/10.1002/2014GL062210.

Novak, L., M. H. P. Ambaum, and B. J. Harvey, 2018: Baroclinic adjustment and dissipative control of storm tracks. *J. Atmos. Sci.*, **75 (9)**, 2955–2970.

Pavan, V., 1996: Sensitivity of a multi-layer quasi-geostrophic β-channel to the vertical structure of the equilibrium meridional temperature gradient. *Quart. J. Roy. Meteor. Soc.*, **122**, 55–72.

Pfeffer, R. L., 1987: Comparison of conventional and transformed in the troposphere. *Quart. J. Roy. Meteor. Soc.*, **113**, 237–254, https://doi.org/10.1002/qj.49711347514.

Ren, H.-L., F.-F. Jin, J.-S. Kug, J.-X. Zhao, and J. Park, 2009: A kinematic mechanism for positive feedback between synoptic eddies and nao. *Geophys. Res. Lett.*, **36**, L11709, https://doi.org/10.1029/2009GL037294.

Rivière, G., 2011: A dynamical interpretation of the poleward shift of the jet streams in global warming scenarios. *J. Atmos. Sci.*, **68**, 1253–1272.

Robert, L., G. Riviere, and F. Codron, 2019: Effect of upper- and lower-level baroclinicity on the persistence of the leading mode of midlatitude jet variability. *J. Atmos. Sci.*, **76 (1)**, 155–169.

Schneider, T., and C. C. Walker, 2008: Scaling laws and regime transitions of macroturbulence in dry atmospheres. *J. Atmos. Sci.*, **65**, 2153–2173.

Shaw, T. A., and Coauthors, 2016: Storm track processes and the opposing influences of climate change. *Nature Geosci*, **9**, 656–664.

Simmons, A. J., and B. J. Hoskins, 1978: The life cycles of some nonlinear baroclinic waves. *J. Atmos. Sci.*, **35**, 411–431.

Accepted for publication in *Journal of the Atmospheric Sciences*. DOI: 10.1175/JAS-D-21-0307.1

Stone, P., 1972: A simplified radiative-dynamical model for the static stability of rotating atmospheres. *J. Atmos. Sci.*, **29**, 405–418.

Stone, P. H., 1978: Baroclinic adjustment. *J. Atmos. Sci.*, **35**, 561–571.

Stone, P. H., and M.-S. Yao, 1987: Development of a Two-Dimensional Zonally Averaged Statistical-Dynamical Model.Part II: The Role of Eddy Momentum Fluxes in the General Circulation and their Parameterization. *J. Atmos. Sci.*, **44**, 3769 – 3786.

Sun, L., G. Chen, and J. Lu, 2013: Sensitivities and mechanisms of the zonal mean atmospheric circulation response to tropical warming. *J. Atmos. Sci.*, **70**, 1569–1586.

Thorncroft, C., B. Hoskins, and M. McIntyre, 1993: Two paradigms of baroclinic-wave life-cycle behaviour. *Quart. J. Roy. Meteor. Soc.*, **119**, 17–55.

Wang, L., and S. Lee, 2016: The role of eddy diffusivity on a poleward jet shift. *J. Atmos. Sci.*, **73**, 4945–4958.

Wang, L., and N. Nakamura, 2015: Covariation of finite-amplitude wave activity and the zonal mean flow in the midlatitude troposphere: 1. Theory and application to the Southern Hemisphere summer. *Geophys. Res. Lett.*, **42**, 8192–8200.

Wu, Y., R. Seager, T. A. Shaw, M. Ting, and N. Naik, 2013: Atmospheric circulation response to an instantaneous doubling of carbon dioxide. Part II: Atmospheric transient adjustment and its dynamics. *J. Climate.*, **26**, 918–935.

Xiao, B., Y. Zhang, X.-Q. Yang, and Y. Nie, 2016: On the role of extratropical air-sea interaction in the persistence of the southern annular mode. *Geophys. Res. Lett.*, **43**, 8806–8814, https://doi.org/10.1002/2016GL070255.

Yuval, J., and Y. Kaspi, 2016: Eddy activity sensitivity to changes in the vertical structure of baroclinicity. *J. Atmos. Sci.*, **73**, 1709–1726.

Yuval, J., and Y. Kaspi, 2017: The effect of vertical baroclinicity concentration on atmospheric macroturbulence scaling relations. *J. Atmos. Sci.*, **74**, 1651–1667.

Yuval, J., and Y. Kaspi, 2020: Eddy activity response to global warming-like temperature changes. *J. Climate.*, **33 (4)**, 1381–1404.

Accepted for publication in *Journal of the Atmospheric Sciences*. DOI 10.1175/JAS-D-21-0307.1

Zhang, Y., P. Stone, and A. Solomon, 2009: The role of boundary layer processes in limiting PV homogenization. *J. Atmos. Sci.*, **66**, 1612–1632.

Zhang, Y., X.-Q. Yang, Y. Nie, and G. Chen, 2012: Annular mode-like variation in a multilayer quasigeostrophic model. *J. Atmos. Sci.*, **69**, 2940–2958.

Zurita-Gotor, P., 2007: The relation between baroclinic adjustment and turbulent diffusion in the two-layer model. *J. Atmos. Sci.*, **64 (4)**, 1284–1300.

Zurita-Gotor, P., and R. Lindzen, 2007: Theories of Baroclinic Adjustment and Eddy Equilibration. *The Global Circulation of the Atmosphere: Phenomena, Theory, Challenges*, T. Schneider, and A. Sobel, Eds., Princeton, NJ: Princeton Univ. Press, 22–46.

Zurita-Gotor, P., and G. Vallis, 2009: Equilibration of baroclinic turbulence in primitive equation and quasi-geostrophic models. *J. Atmos. Sci.*, **66**, 837–863.

Zurita-Gotor, P., and G. K. Vallis, 2010: Circulation sensitivity to heating in a simple model of baroclinic turbulence. *J. Atmos. Sci.*, **67 (5)**, 1543–1558.

Accepted for publication in *Journal of the Atmospheric Sciences*. DOI 10.1175/JAS-D-21-0307.1